

# Molecularly imprinted titania microbeads for extraction of the metabolite 1-hydroxypyrene from urine prior to its determination by HPLC

Do-Hyeon Yang<sup>1</sup> · Min Jae Shin<sup>2</sup> · Minhee Kim<sup>1</sup> · Yong-Dae Kim<sup>3</sup> · Heon Kim<sup>3</sup> · Jae Sup Shin<sup>1</sup>

Received: 7 December 2015 / Accepted: 8 February 2016 / Published online: 29 February 2016  
© Springer-Verlag Wien 2016

**Abstract** The authors describe a method for the extraction of 1-hydroxypyrene (1-OHP) from urine by using a molecularly imprinted TiO<sub>2</sub> gel, and the determination of 1-OHP by HPLC. This method was applied to determine levels of 1-OHP in urine of patients in order to estimate the degree of exposure to polycyclic aromatic hydrocarbons. The molecularly imprinted TiO<sub>2</sub> gel (MITiG) was prepared by polycondensation of titanium(IV) butoxide in the presence of the template 1-OHP. The gel was deposited in the form of a thin film on a quartz support, and the 1-OHP template was eluted. The resulting MITiG binds 1-OHP much better than chemically related species. The MITiG was then applied to prepare micro beads (with a typical diameter of 500–600 μm) to enlarge the specific surface. These beads were used to extract 1-OHP from urine. Following elution of 1-OHP with ethanol, it was quantified by HPLC with fluorescence detection at excitation/emission wavelengths of 242/388 nm. The method is accurate, cheaper and faster than the often used enzyme-based method.

**Keywords** Polycyclic aromatic hydrocarbons · Titania sol-gel · Nanoporous material · Clinical assay · Chromatography · Fluorescence detection · SEM

## Introduction

Polycyclic aromatic hydrocarbons (PAHs), which are formed during the incomplete combustion of fossil fuels, are widely distributed in our environment [1, 2]. Human exposure to PAHs may occur through smoking, polluted air, food consumption, and occupational contact. Many of them are considered to be dangerous environmental contaminants with mutagenic and carcinogenic properties. Urinary 1-hydroxypyrene (1-OHP), a major metabolite of pyrene, has been shown to exhibit a good relationship with PAH exposure in various organisms; thus, it has been used as a biomarker in a number of studies to monitor human exposure to PAHs [3–7].

There are several methods to detect urinary 1-OHP. Among them, the practical and representative method used in hospitals until now is the one reported by Jongeneelen in 1987 [3]. At the Chungbuk National University Hospital, his method has been used to detect a patient's urinary 1-OHP until now [5].

It is very difficult to detect urinary 1-OHP, because the concentration of 1-OHP in urine is very low and it exists in urine together with its several ester forms. Therefore, in Jongeneelen's method, enzymes such as β-glucuronidase and arylsulfatase are used for the hydrolysis of the ester forms to increase the amount of 1-OHP in urine, and high-performance liquid chromatography (HPLC) is then used to detect 1-OHP [3]. However, these enzymes are very expensive and it takes more than 16 h for the hydrolysis of the ester forms. Therefore, a cheaper, faster, and simpler method for the detection of urinary 1-OHP is required.

**Electronic supplementary material** The online version of this article (doi:10.1007/s00604-016-1787-6) contains supplementary material, which is available to authorized users.

✉ Jae Sup Shin  
jsshin@chungbuk.ac.kr

- <sup>1</sup> Department of Chemistry, Chungbuk National University, Cheongju, Chungbuk 28644, South Korea
- <sup>2</sup> Department of Chemical and Biomolecular Engineering, Korea Advanced Institute of Science and Technology, Daejeon 34141, South Korea
- <sup>3</sup> Department of Preventive Medicine, Chungbuk National University, Cheongju, Chungbuk 28644, South Korea

Molecular imprinting is a technique to create artificial receptors which show mimic biological molecular recognition phenomena [8–12]. This technique is based on the self-assembly of certain components needed for imprinting, such as templates, functional monomers, and cross-linking monomers to create a polymer matrix. The template molecule is then removed from the matrix under certain conditions, leaving behind a cavity complementary in size and shape to the template. The obtained cavity can function as a selective binding site for a specific template molecule. Molecular imprinting materials have a wide range of practical applications such as for separation, enzyme mimicking, chemical sensing, and biosensing [13–16]. In general, organic matrices [17–20] using cross-linked polymers, and inorganic matrices [21–24] such as silica and titania prepared using sol–gel technology are widely used for molecular imprinting. Although organic matrices are dominant, inorganic matrices have attracted practical interests because of their easy control and simple deposition onto surfaces. In particular, imprinted inorganic thin films have been applied to sensor transducers because binding sites for a specific template molecule are not far from the surface and ready access of template molecules to binding sites is encouraged [25, 26]. In our previous studies, we have demonstrated the advantages of TiO<sub>2</sub> gel thin films as useful matrices for molecular imprinting; moreover, molecularly imprinted TiO<sub>2</sub> gel matrices showed good recognition properties with high sensitivity and selectivity to target analytes [27–30].

Over the last decade, various approaches to develop PAH-imprinted polymer matrices have been proposed. Dickert et al. reported PAH-imprinted polymers developed using cross-linked polyurethanes, in which the chemical structure of the imprinted molecule determines its selectivity [31, 32]. Kirsch et al. reported a molecular imprinting system for 1-OHP based on divinylbenzene and styrene, in which binding occurred only on the basis of hydrophobic interactions [33]. Knopp et al. reported six kinds of molecularly imprinted polymers (MIPs) or microspheres for benzopyrene. MIPs using 4-vinylpyridine and divinylbenzene as functional and cross-linking monomers showed good recognition toward benzopyrene in water and coffee samples [34]. Krupadam et al. reported an MIP-particle adsorbent for carcinogenic PAHs developed via a non-covalent templating technique by using methacrylic acid as the functional monomer, and ethylene glycol dimethacrylate as the cross-linker [35]. MIP particles exhibited significant binding affinity toward PAHs even in the presence of environmental parameters. Song et al. [36] and Guo et al. [37] reported a new kind of inorganic MIP adsorbent for PAHs prepared on the basis of a covalent/non-covalent hybrid strategy by using sol–gel technology.

Research on molecular imprinting started with studies on a model enzyme reaction system. The most important advantage of molecular imprinting over enzyme systems is that it can be used under diverse conditions such as different

temperatures, pH values, and solvents. However, a major drawback of molecular imprinting is that selectivity and turnover rate are lower than those in the case of enzyme systems. In particular, slow turnover rate is a great obstacle to molecular imprinting research. A slow turnover rate arises when the substrate is separated from cavities very slowly during molecular imprinting. Therefore, we used a molecular imprinting system as a tool for collecting 1-OHP. On the basis of this strategy, we developed a new method for detecting urinary 1-OHP without using expensive enzymes or a long pretreatment time. Our method was used to successfully detect urinary 1-OHP at the Chungbuk National University Hospital. In this paper, this novel method is introduced and explained.

## Experimental

### Materials and instruments

Titanium(IV) butoxide (TIBU) was purchased from Acros Organics, USA. Pyrene, 1-hydroxypyrene (1-OHP), 1-pyrenecarboxylic acid (PYCA), and 1-pyrenebutyric acid (PYBA) were obtained from Aldrich, USA (<http://www.sigmaaldrich.com/korea.html>). Naphthalene, 2-naphthol, anthracene, and 2-anthracenecarboxylic acid (ANCA) were purchased from Tokyo Kasei, Japan (<http://www.tcichemicals.com/en/jp/index.html>). Structures of chemicals used in this study are shown in Supporting Information Figure S4. Deionized pure water (18.3 M $\Omega$  cm) was obtained by reverse osmosis followed by ion exchange and filtration (AquaMax™-Ultra, Younglin Instrument, Korea, <http://www.younglin.com>). The bead (Trilite AW90) was obtained from Samyang Co., Korea (<http://www.samyangcorp.com>). Trilite AW90, which is a weakly basic anionic exchange resin, was prepared using polystyrene and divinylbenzene. The bead size was 400–720  $\mu$ m, and above 95 % was 500–600  $\mu$ m, and the homogeneity was less than 1.2. The density of the bead was 640 g·L<sup>-1</sup>.

The scanning electron microscopy (SEM) analysis was performed using both Hitachi S-2500C and Hitachi S-5200 V scanning electron microscopes (<http://www.hitachi.com>).

### Molecular imprinting on quartz plates

Titanium(IV) butoxide (TIBU) was used as a precursor of the TiO<sub>2</sub> matrix, and 1-OHP was used as a template molecule in toluene/ethanol (1:1, v/v). This mixture was used for the preparation of molecularly imprinted films. In order to determine imprinting conditions in detail, the 1-OHP concentration in the mixture was varied from 0 to 20 mM against 200 mM TIBU. Only the 200 mM TIBU solution was used for the non-imprinted film. Prior to film deposition, a quartz plate was cleaned with concentrated sulfuric acid (96 %) and thoroughly washed with deionized pure water. This was followed

by sonication (Branson 2210, USA, <https://www.bransoninc.com>) treatment with 1 wt% ethanolic KOH (ethanol/water =3:2, v/v) for 30 min, washing with ethanol and water, and finally drying by flushing N<sub>2</sub> gas. The films were prepared by spin-coating for 30 s at 4000 rpm (358 g) with 10 μL of the film-forming stock solution on quartz plates under a N<sub>2</sub> atmosphere by using a YS-100D spin-coater system (Yooil Engineering, Korea, <http://www.yiengineering.com>). The films were then allowed to undergo hydrolysis and sol–gel reactions in a 90 % humidity chamber at 25 °C for 12 h.

To remove template molecules, the prepared films were immersed in ethanol for 20 min at 25 °C, thoroughly rinsed with water three times, and dried using N<sub>2</sub> gas. This treatment led to the removal of template molecules, and resulted in the formation of imprinted cavities in the TiO<sub>2</sub> gel films. Their removal was confirmed by characteristic UV absorption peaks for 1-OHP. UV absorption spectra were obtained using a Lambda 35 UV spectrophotometer, PerkinElmer (<http://www.perkinelmer.com>). Guest binding of 1-OHP and other molecules to the imprinted and non-imprinted films was conducted under the same conditions. Films were incubated in 0.10 mM guest molecules in a 50 % aqueous methanol solution at room temperature for 30 min, thoroughly rinsed with water three times, and dried in a stream of N<sub>2</sub> gas.

### Molecular imprinting on bead

TIBU (1.360 g, 4.00 mmol) and 1-OHP (0.0681 g, 0.200 mmol) were added to 20 mL of a mixed solution of ethanol and toluene (1:1, v/v). This solution was stirred for 3 h at 25 °C. Ten grams of the bead was added to the solution and stirred for 1 h at 25 °C. The bead was then collected and dried using N<sub>2</sub> gas for 3 h. It was then allowed to undergo hydrolysis and sol–gel reactions in a 90 % humidity chamber at 25 °C for 12 h. To remove template molecules, the prepared bead was immersed in 100 mL of ethanol for 30 min at 25 °C, thoroughly rinsed with pure water and ethanol, and dried using N<sub>2</sub> gas.

### Detection of 1-OHP in human urine

Hundred milligrams of the 1-OHP-imprinted bead was conditioned with 1.0 mL of a 50 % methanol solution in a 10 mL tube. A solution of 1.0 mL human urine and 1.0 mL methanol was added to the tube, and the resultant mixture was incubated for 4 h. The bead was then washed with 10 mL of water, and was extracted with 1.0 mL of ethanol for 1 h.

A high-performance liquid chromatography (HPLC) system (Hitachi, Tokyo, Japan), consisting of a pump (L-2130), a fluorescence detector (L-7485), and an automatic injector (L-7200), was used. A 150-mm reverse phase column (TSK gel ODS-80TM, Tosoh, Tokyo, Japan) was used for analysis. The mobile phase was an 80 % methanol solution. The flow rate

was 0.8 mL·min<sup>-1</sup>. Excitation/emission wavelengths used in the detection were 242/388 nm.

## Results and discussion

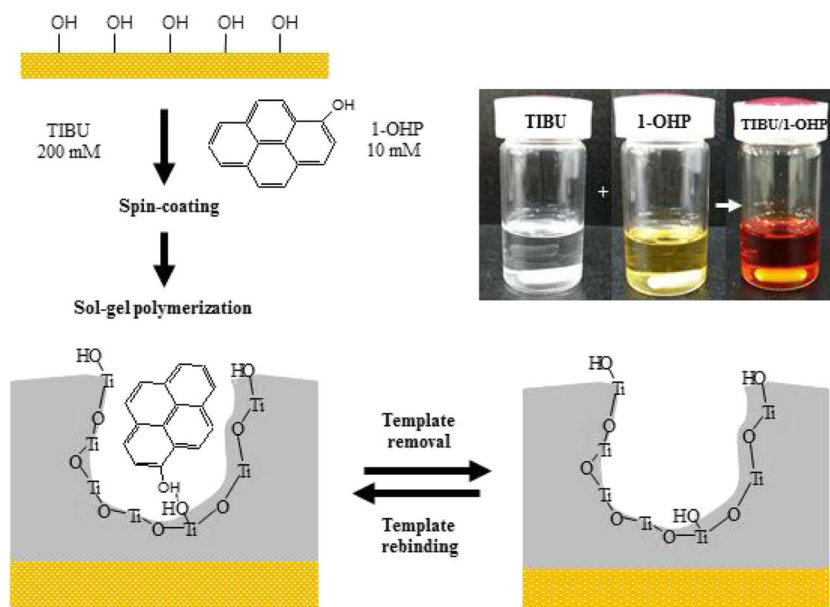
### Molecular imprinting on quartz plates

The molecular imprinting was conducted usually using the organic polymers as basic compounds. Recently, inorganic polymers such as silicone oxide and titanium oxide were tried to use as the basic compounds for molecular imprinting. Silicone oxide was used more frequently than titanium oxide because many kinds of the monomeric compounds for the silicone oxide were existed. But we chose titanium oxide because the thin membrane using titanium oxide can be formed more easily than silicone oxide.

In the first stage of this study, we attempted molecular imprinting on quartz plates because the UV spectrum was directly obtained; therefore, the extent of binding and removal of substrates was easily estimated. Figure 1 shows a schematic illustration of the molecular imprinting and rebinding procedure for 1-OHP in TiO<sub>2</sub> gel matrices; in addition, it also shows a photograph of the stock solutions used: a) 200 mM TIBU, b) 10 mM 1-OHP, and c) a mixed solution of 200 mM TIBU and 10 mM 1-OHP. TIBU and 1-OHP solutions were colorless and pale yellow, respectively. However, the mixed solution was deep orange in color. This deep orange color was due to the formation of a complex of TIBU and 1-OHP. These solutions were deposited by spin-coating on a quartz plates, and a 1-OHP template was embedded in TiO<sub>2</sub> gel matrices via a sol–gel reaction. The sol–gel reaction was carried out in a 90 % humidity chamber. After the completion of this reaction, the 1-OHP template was removed via ethanol treatment. After template removal, the remaining cavities provided specific binding sites for 1-OHP in TiO<sub>2</sub> gel matrices.

Figure 2a and 2b show UV absorption spectra changes at 242 nm due to the removal and rebinding of 1-OHP, respectively, on the quartz plates. All the UV spectra are shown in Supporting Information Fig. 1S. The maximum absorbance of 1-OHP at 242 nm decreased rapidly upon incubation in ethanol. Eventually, the 1-OHP template in the TiO<sub>2</sub> gel matrix was completely removed within 10 min. The UV spectrum of the film corresponding to after 1-OHP template removal showed only TiO<sub>2</sub> gel absorption, indicating that the template molecules were completely removed from the TiO<sub>2</sub> gel matrix. In the rebinding experiment, the maximum absorbance of 1-OHP at 242 nm increased rapidly within 10 min. This observation indicated that 1-OHP binding occurred well in the rebinding process. In the removal process, the absorbance at 242 nm decreased to -0.248; further, in the first rebinding process, the absorbance at 242 nm increased to 0.267. These values were recorded during the seven repetitions of removal

**Fig. 1** A schematic illustration for molecular imprinting and rebinding procedure of a 1-OHP template in TiO<sub>2</sub> gel matrices, and a photograph of stock solutions

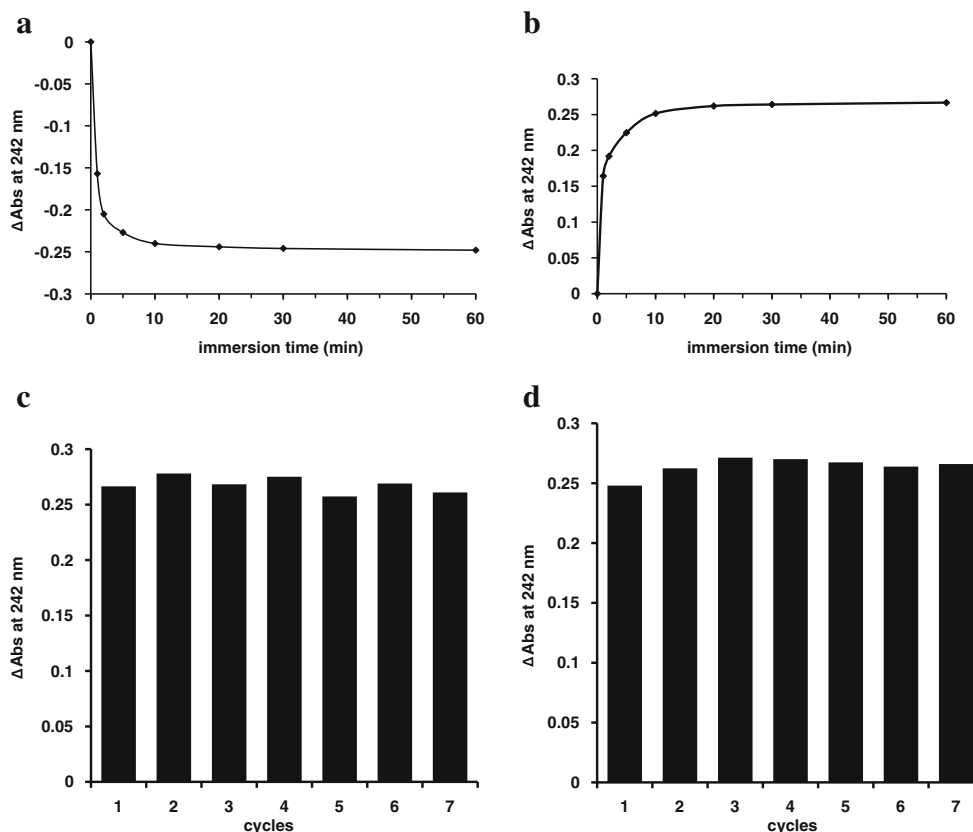


and rebinding processes, and are shown in Fig. 2c and d, respectively. In the seven repetitions of the rebinding process, the average value of absorbance at 242 nm was  $0.267 \pm 0.0063$ ; in the seven repetitions of the removal process, the average value was  $-0.264 \pm 0.0067$ . Thus, almost an equal value was observed in both the removal and rebinding

processes. This indicates that the two processes occurred repeatedly in exactly the same manner.

The removal and rebinding processes were also investigated by IR spectroscopy. The procedure is shown in Supporting Information, and the results are shown in Supporting Information Fig. 2S.

**Fig. 2** **a** UV absorption changes at 242 nm with time due to 1-OHP removal from the imprinted film. **b** UV absorption changes at 242 nm with time due to 1-OHP rebinding with the imprinted film. **c** UV absorption increase for re-bound 1-OHP at 242 nm during the repeated rebinding process. **d** UV absorption decrease for removed 1-OHP at 242 nm during the repeated removal process



The surface morphology of the 1-OHP-imprinted films was investigated from micrographs on the basis of atomic force microscopy (AFM) measurements. The results are shown in Supporting Information Fig. 3S. AFM micrographs indicated that the films scarcely showed a change in their overall morphology before and after template removal. The film surfaces were extremely smooth and uniform over large areas with a root mean square roughness of 0.211 nm and 0.240 nm before and after template removal, respectively.

In order to determine the optimal imprinting conditions for preparing 1-OHP-imprinted TiO<sub>2</sub> gel plate, the template concentration in the mixture was varied from 0 to 20 mM against 200 mM TIBU. Figure 3a shows the UV spectrum of the plate after 1-OHP rebinding according to the 1-OHP template concentration for molecular imprinting. An increased UV absorbance value was observed at 242 nm, as shown in Fig. 3b. The figure shows a bell shape profile for the curve, and the maximum UV absorbance increase was observed at a 1-OHP template concentration of 10 mM. These results can be explained on the basis of Fig. 4. The number of binding sites increased with increasing template concentration. However, when the template concentration was increased beyond the optimum value, the template molecules overlapped (Fig. 4). The extent of binding could be reduced by forming such overlapped sites.

It was concluded that 10 mM was the optimum value of the 1-OHP template concentration against 200 mM of TIBU for achieving maximum 1-OHP binding.

Generally, during molecular imprinting, nonspecific binding occurs along with specific binding. Therefore, we prepared a non-imprinted film and estimated the extent of nonspecific binding. The results are shown in Fig. 3c. The UV absorbance increase at 242 nm for the non-imprinted plate was 0.11, whereas that for the 1-OHP-imprinted plate was 0.27. This large difference indicated that imprinted sites were formed on the latter plate.

### Guest selectivity

The guest binding and selectivity of 1-OHP-imprinted plates prepared using 10 mM template and 200 mM TIBU were determined by UV spectroscopy measurements. The absorption coefficient of each analyte used in the binding study was estimated. All guest molecules were subjected to the intrinsically same guest binding process. The binding density (mol cm<sup>-2</sup>) of all guest molecules on each imprinted film was calculated from their molecular extinction coefficients, and the relative binding efficiency was defined as the molar ratio of the bound guest and template molecules ( $\nu_{\text{guest}}/\nu_{\text{template}}$ ). The results for relative

**Fig. 3** **a** UV absorption for 1-OHP-imprinted film after 1-OHP binding, **b**  $\Delta$ Abs at 242 nm for 1-OHP binding according to 1-OHP template concentration, **c**  $\Delta$ Abs at 242 nm for 1-OHP binding to (1) non-imprinted film, and (2) 1-OHP-imprinted film

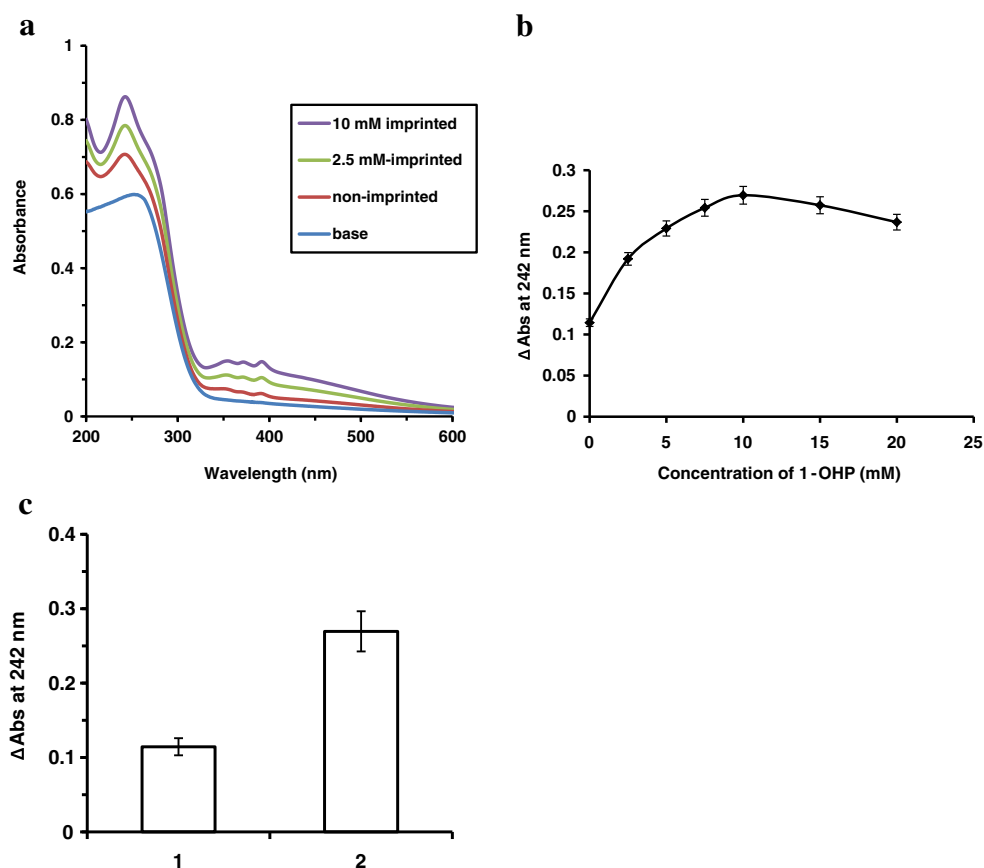
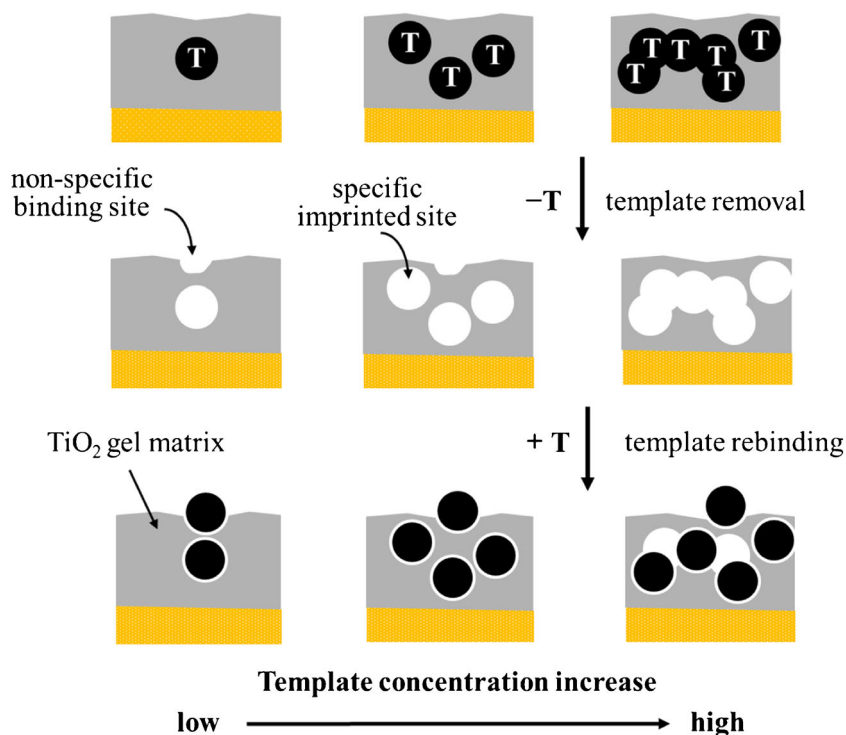




**Fig. 4** Schematic illustrations of TiO<sub>2</sub>-gel imprinted sites according to template concentration



binding are listed in Table 1. The 1-OHP-imprinted plate showed higher selectivity toward 1-OHP than toward other guest molecules. The binding efficiency of the 1-OHP-imprinted plate decreased in the following order: 1-OHP > 1-pyrenecarboxylic acid (PYCA) > 2-naphthol > 2-anthracenecarboxylic acid (ANCA) > 1-pyrenebutyric acid (PYBA) > pyrene > naphthalene > anthracene. Guest molecules that possess a hydroxyl (2-naphthol) or carboxylic functional group (PYCA, ANCA, and PYBA) showed relatively higher binding efficiency than pyrene, naphthalene, and anthracene, which only possess an aromatic ring.

#### Molecular imprinting on bead

Using the data obtained from 1-OHP-imprinted plates, molecular imprinting was conducted on a bead for detecting the 1-OHP amount in human urine. The reason for selecting a bead was to enlarge the imprinted surface area. We considered that an enlarged surface area would be helpful in exactly detecting the 1-OHP amount in human urine. We conducted 1-OHP imprinting on the bead under the same conditions employed in the previous experiment for plates. After 1-OHP imprinting on the bead, SEM images were obtained and are shown in Fig. 5a. The coating surface can be observed in the SEM image; a

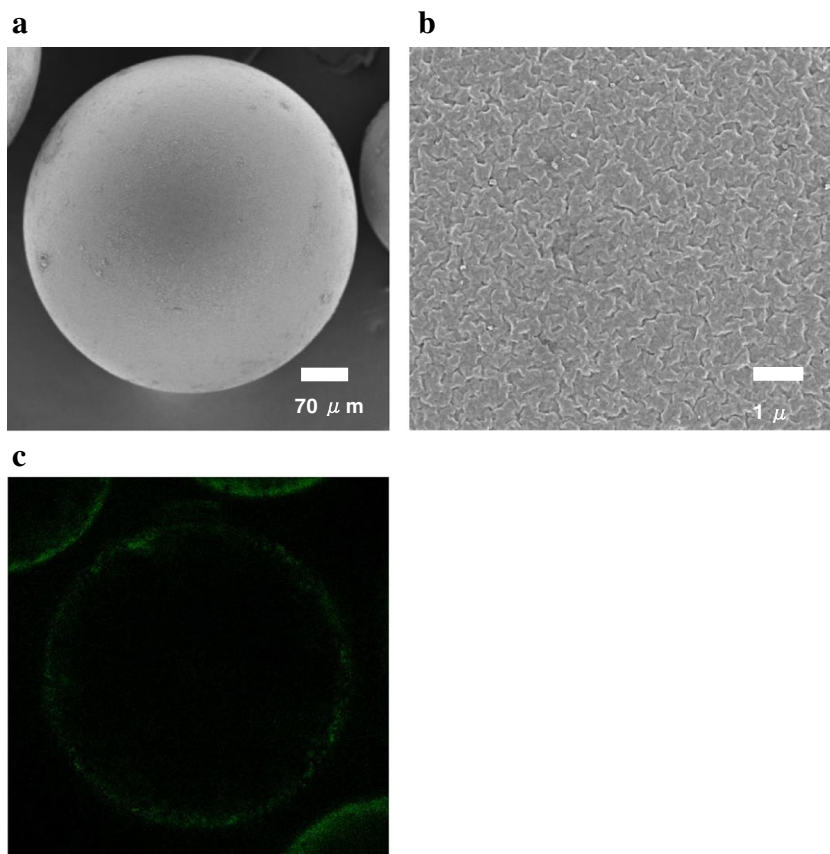
**Table 1** Relative binding efficiency of 1-OHP-imprinted film for guest molecules

Guest	$\lambda_{\max}$ (nm)	$\epsilon^a$ (cm <sup>-1</sup> M <sup>-1</sup> )	$\Delta$ Abs	Binding density (M cm)	Relative binding efficiency <sup>b</sup>
1-OHP	242	40,780	0.269	$6.60 \times 10^{-6}$	1.00
Pyrene	240	59,330	0.0101	$1.70 \times 10^{-7}$	0.026
Naphthalene	220	85,050	0.012	$1.41 \times 10^{-7}$	0.021
2-naphthol	225	68,430	0.174	$2.54 \times 10^{-6}$	0.38
Anthracene	252	179,040	0.0102	$5.60 \times 10^{-8}$	0.0085
ANCA	258	89,520	0.239	$2.67 \times 10^{-6}$	0.40
PYBA	242	60,320	0.0761	$1.26 \times 10^{-6}$	0.19
PYCA	243	46,490	0.142	$3.05 \times 10^{-6}$	0.46

<sup>a</sup> Absorption coefficient

<sup>b</sup> Relative binding efficiency of each analyte defined as the molar ratio of bound guest to bound 1-OHP

**Fig. 5** **a** SEM image of 1-OHP-imprinted bead, **b** SEM image of the surface of 1-OHP-imprinted bead, and **c** confocal image of 1-OHP-imprinted bead after 1-OHP rebinding



wrinkled pattern that was formed during the sol–gel reaction can be observed in the enlarged image (Fig. 5b).

A confocal image for the 1-OHP-imprinted bead obtained after 1-OHP rebinding is shown in Fig. 5c. The fluorescence at the surface of the bead is due to the rebound 1-OHP.

### Detecting 1-OHP in urine

The purpose of this study is to introduce a new method for detecting 1-OHP in urine that is cheaper and simpler than previously used methods. First, we check that the prepared

1-OHP-imprinted bead can be used to detect 1-OHP. For this, 100 mg of the prepared bead was incubated in a 1.0 mL 50 % aqueous methanol solution containing 10.0 ng of 1-OHP for 3 h. The bead was then washed with water three times. Thereafter, the bead was extracted using 1 mL of ethanol for 1 h, and the amount of recovered 1-OHP in ethanol was estimated by HPLC. The results showed that the average recovered amount of 1-OHP in seven repeated experiments was  $9.81 \pm 0.22$  ng. The detailed data are shown in Supporting Information Table 1S. The results show that 98.1 % of 1-OHP was recovered.

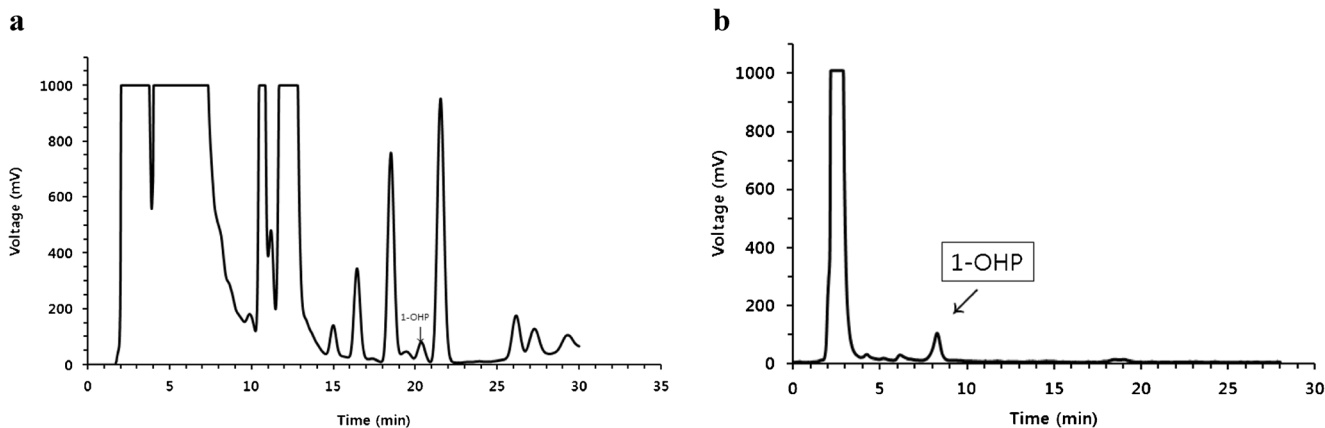


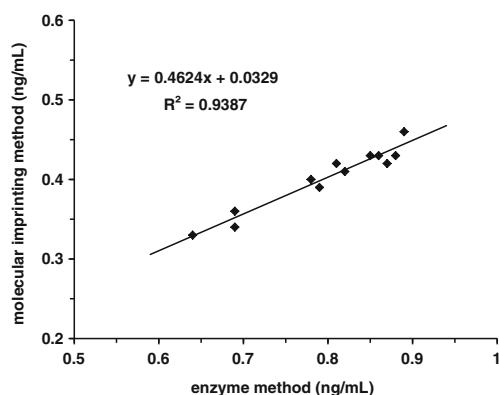
**Fig. 6** HPLC results for 1-OHP measurement in urine for a) enzyme-based method, and b) molecular imprinting method

**Table 2** Urinary 1-OHP level measured by molecular imprinting method and enzyme-based method

Sample No	Enzyme method	Molecular imprinting method
1	0.82	0.39
2	0.81	0.44
3	0.79	0.48
4	0.88	0.52
5	1.29	0.63
6	1.39	0.68
7	1.38	0.76
8	1.57	0.78
9	1.71	0.83
10	1.73	0.86
11	1.80	0.91
12	1.79	0.93

In the next experiment, PYCA, 2-naphthol, ANCA, PYBA, pyrene, naphthalene, anthracene, and 1-OHP (5.0 ng of each) were incubated with 100 mg of the 1-OHP-imprinted bead in a 1.0 mL 50 % aqueous methanol solution for 3 h. The bead was then extracted using 1 mL of ethanol for 1 h. The amount of recovered 1-OHP in ethanol was estimated by HPLC. The results showed that the average recovered amount of 1-OHP in seven repeated experiments was  $4.71 \pm 0.08$  ng. The detailed data are shown in Supporting Information Table 2S. The results indicate that 94.2 % of 1-OHP was recovered. This value is slightly lower than the previous result; however, 94.2 % can still be considered a significant value.

In the next experiment, we attempted to use the imprinted bead to detect 1-OHP in human urine. The obtained results were compared with those obtained using an enzyme-based method [5]. The enzyme-based method was used at the Chungbuk National University before our method was introduced. The obtained HPLC profiles are compared in Fig. 6. Figure 6a and b show the results for the enzyme-based method and our method using the 1-OHP-imprinted bead,

**Fig. 7** Comparison of 1-OHP concentration in the case of molecular imprinting method and enzyme-based method

respectively. In Fig. 6a, many peaks can be observed in the HPLC profile; moreover, the 1-OHP peak is positioned between large peaks. However, in Fig. 6b, not many peaks are observed; therefore, the 1-OHP peak can be observed very clearly.

The amount of 1-OHP was estimated using both our method and the enzyme-based method in 12 urine samples. The results are shown in Table 2. In order to determine the correlation between the two methods, plotting results are shown in Fig. 7. In this figure, the correlation coefficient is 0.939. This value indicates that the efficiency of our method is comparable to that of the enzyme-based method.

The 1-OHP amount estimated using our method is relevant to 46 % of that estimated using the enzyme-based method. In the human body, pyrene is changed to 1-OHP and its ester forms via a metabolic process. In the enzyme-based method, some ester forms were changed to 1-OHP by reacting with the enzyme. Because the amount of pure 1-OHP in urine is very small, hydrolyzing enzymes must be used in the enzyme-based method to increase the 1-OHP amount. In contrast, in the case of our method, in which no enzymes are used, a clear 1-OHP peak was observed in the HPLC profile without supporting the hydrolyzing enzymes.

In conclusion, an easy and cheap method for detecting 1-OHP in urine without using enzymes and a long time pretreatment process was introduced in this paper. But in order to be used for 1-OHP detection more frequently at many organizations, our method must be standardized for mass production. Especially the coating technique to control the coating thickness had to be studied for mass production. It will be studied next time.

## Conclusions

As a basic experiment, 1-OHP-imprinted  $\text{TiO}_2$  gel films were fabricated and used for detecting 1-OHP. These films showed good guest selectivity and binding affinity to 1-OHP comparing with other similar organic molecules, whose relative binding efficiencies were 0.0085–0.46. The obtained results were utilized to use bead materials for practically detecting 1-OHP in urine. The bead showed good extraction ability for 1-OHP in artificial samples which contained 10.0 ng of 1-OHP in 1.0 mL solution, or contained 1-OHP and other similar organic molecules (5.0 ng of each) in 1.0 mL solution. Finally, this bead was used for detecting 1-OHP in urine of 12 persons. Our method showed the comparable 1-OHP detecting results comparing with the enzyme-based method. Our method is cheaper and simpler than the enzyme-based method for 1-OHP detection.

**Compliance with ethical standard** The authors declare that they have no competing interests.



## References

- Hemminki K, Veidebaum T (1999) Environmental pollution and human exposure to polycyclic aromatic hydrocarbons in the East Baltic region. *Scand J Work Environ Health* 25:33–39
- Lijinsky W (1991) The formation and occurrence of polynuclear aromatic hydrocarbons associated with food. *Mutat Res* 259:251–261
- Jongeneelen FJ, Anzion RB, Henderson PT (1987) Determination of hydroxylated metabolites of polycyclic aromatic hydrocarbons in urine. *J Chromatogr* 413:227–232
- Schere G, Frank S, Riedel K, Meger-Kossien I, Renner T (2000) Biomonitoring of exposure to polycyclic aromatic hydrocarbons of nonoccupationally exposed persons. *Cancer Epidemiol Biomark Preve* 9:373–380
- Kim H, Cho S-H, Kang J-W, Kim Y-D, Nan H-M, Lee C-H, Lee H, Kawamoto T (2000) Urinary 1-hydroxypyrene and 2-naphthol concentrations in male Koreans. *Int Arch Occup Environ Health* 74: 59–82
- Kishikawaa N, Wadaa M, Kurodaa N, Akiyamab S, Nakashimac K (2003) Determination of polycyclic aromatic hydrocarbons in milk samples by high-performance liquid chromatography with fluorescence detection. *J Chromatogr B* 789:257–264
- Cooper JA (1980) Environmental impact of residential wood combustion emissions and its implications. *J Air Poll Cont Assoc* 30: 855–861
- Wulff G (2002) Enzyme-like catalysis by molecularly imprinted polymer. *Chem Rev* 102:1–27
- Haupt K, Mosbach K (2000) Molecularly imprinted polymers and their use in biomimetic sensors. *Chem Rev* 100:2495–2504
- Selyanchyn R, Lee S-W (2013) Molecularly imprinted polystyrene-titanium hybrids with both ionic and  $\pi$ - $\pi$  interactions: a case study with pyrenebutyric acid. *Microchim Acta* 180:1443–1452
- Aziz-Zanjani MO, Mehdinia A (2014) A review on procedures for the preparation of coatings for solid phase microextraction. *Microchim Acta* 181:1169–1190
- Wulff G (2013) Forty years of molecular imprinting in synthetic polymers: origin, features and perspectives. *Microchim Acta* 180: 1359–1370
- Yang D-H, Ju M-J, Maeda K, Hayashi K, Toko K, Lee S-W, Kunitake T (2006) Design of highly efficient receptor sites by combination of cyclodextrin units and molecular cavity in TiO<sub>2</sub> ultrathin layer. *Biosens Bioelectron* 22:388–392
- Ju M-J, Yang D-H, Takahara N, Hayashi K, Toko K, Lee S-W, Kunitake T (2007) Landmine detection: improved binding of 2,4-dinitrotoluene CyD/metal oxide matrix and its sensitive detection via a cyclic surface-polarization impedance (cSPI) method. *Chem Comm* 44:2630–2632
- Shen X, Zhn L, Wang N, Ye L, Tang H (2012) Molecular imprinting for removing highly toxic organic pollutants. *Chem Comm* 48: 788–798
- Shiomi T, Matsui M, Mizukami F, Skakguchi K (2005) A method for the molecular imprinting of hemoglobin on silica surfaces using silanes. *Biomaterials* 26:5564–5571
- Whitcombe MJ, Vulfson EN (2001) Imprinted polymers. *Adv Mater* 13:467–478
- Takeda K, Kuwahara A, Ohmori K, Takeuchi T (2009) Molecularly imprinted tunable binding sites based on conjugated prosthetic groups and ion-paired cofactors. *J Am Chem Soc* 131:8833–8838
- Dirion B, Cobb Z, Schillinger E, Anderson LI, Sellergren B (2003) Water-compatible molecularly imprinted polymers obtained via high-throughput synthesis and experimental design. *J Am Chem Soc* 125:15101–15109
- Hishiyama T, Asanuma H, Komiyama M (2002) Spectroscopic anatomy of molecular-imprinting of cyclodextrin. Evidence for Preferential Formation of Ordered Cyclodextrin Assemblies *J Am Chem Soc* 124:570–575
- Katz A, Davis ME (2000) Molecular imprinting of bulk, microporous silica. *Nature* 403:286–289
- Fireman-Shoresh S, Avnir D, Marx S (2003) General method for chiral imprinting of sol-gel thin films exhibiting enantioselectivity. *Chem Mater* 15:3607–3613
- Lahav M, Kharitonov AB, Willner I (2001) Imprinting of chiral molecular recognition sites in thin TiO<sub>2</sub> films associated with field-effect transistors: novel functionalized devices for chiroselective and chiro-specific analyses. *Chem Eur J* 7:3992–3997
- Lee S-W, Yang D-H, Kunitake T (2005) Regioselective imprinting of anthracene carboxylic acids onto TiO<sub>2</sub> gel ultrathin films: an approach to thin film sensor. *Sensor Actuat B* 104:35–42
- Yang D-H, Ju M-J, Maeda A, Lee S-W (2008) Enhanced sensor capability of juxtaposed  $\beta$ -cyclodextrin rings in TiO<sub>2</sub> ultrathin matrix as determined by cyclic surface-polarization impedance measurement. *Sen Mater* 20:191–200
- Mixutani N, Yang D-H, Selyanchyn R, Korposh S, Lee S-W, Kunitake T (2011) Remarkable enantioselectivity of molecularly imprinted TiO<sub>2</sub> nano-thin films. *Anal Chim Acta* 694:142–150
- Yang D-H, Ham YR, Oh MH, Yoon YS, Shin JS, Kim Y-D, Kim H (2009) Simple method for the fabrication of 1-hydroxypyrene-imprinted TiO<sub>2</sub> gel nano-films. *Curr Appl Phys* 9:e136–e139
- Yang D-H, Takahara N, Lee S-W, Kunitake T (2008) Fabrication of glucose TiO<sub>2</sub> ultrathin films by molecular imprinting and selective detection of monosaccharides. *Sensor Actuat B* 130:379–385
- Yang D-H, Lee S-W, Kunitake T (2005) Facile fabrication of molecularly imprinted cavities in spin-coated TiO<sub>2</sub> nanofilms. *Chem Lett* 34:1686–1687
- Araki K, Yang D-H, Wang T, Selyanchyn R, Lee S-W, Kunitake T (2013) Self-assembly and imprinting of macrocyclic molecules in layer-by-layered TiO<sub>2</sub> ultrathin films. *Anal Chim Acta* 779:72–81
- Dickert FL, Bensenbock H, Tortschanoff M (1998) Molecular imprinting through van der Waals interactions: Fluorescence detection of PAHs in water. *Adv Mater* 10:149–151
- Dickert FL, Hayden O, Halikias KP (2001) Synthetic receptors as sensor coatings for molecules and living cells. *Analyst* 126:766–771
- Kirsch N, Hart JP, Bird DJ, Luxton RW, McCalley DV (2001) Towards the development of molecularly imprinted polymer based screen-printed sensors for metabolites of PAHs. *Analyst* 126:1936–1941
- Lai J-P, Niessner R, Knopp D (2004) Benzo[a]pyrene imprinted polymers: synthesis, characterization and SPE application in water and coffee samples. *Anal Chim Acta* 522:137–144
- Krupadam RJ, Khan MS, Wate SR (2010) Removal of probable human carcinogenic polycyclic aromatic hydrocarbons from contaminated water using molecularly imprinted polymer. *Water Reserch* 44:681–688
- Song X, Li J, Xu S, Ying R, Mac J, Liao C, Liu D, Yu J, Chen J (2012) Determination of 16 polycyclic aromatic hydrocarbons in seawater using molecularly imprinted solid-phase extraction coupled with gas chromatography-mass spectrometry. *Talanta* 99: 75–82
- Guo L, Zeng Y, Guan A, Chen G (2011) Preparation and characterization of molecularly imprinted silica particles for selective adsorption of naphthalene. *React Funct Polym* 71:1172–1176